Neuro-Oncology 15(9):1200–1211, 2013.
doi:10.1093/neuonc/not054
Advance Access publication May 30, 2013

The soluble form of the tumor suppressor Lrig1 potently inhibits in vivo glioma growth irrespective of EGF receptor status

Mikael Johansson†, Anaïs Oudin†, Katja Tiemann, Amandine Bernard, Anna Golebiewska, Olivier Keunen, Fred Fack, Daniel Stieber, Baofeng Wang, Håkan Hedman, and Simone P. Niclou

NorLux Neuro-Oncology Laboratory, Department of Oncology, Centre de Recherche Public de la Santé, Luxembourg, Luxembourg (M.J., A.O., K.T., A.B., O.K., F.F., A.G., D.S., S.P.N.); Department of Radiation Sciences, Oncology, Umeå University, Umeå, Sweden (M.J., B.W., H.H.)

Background. Deregulated growth factor signaling is a major driving force in the initiation and progression of glioblastoma. The tumor suppressor and stem cell marker Lrig1 is a negative regulator of the epidermal growth factor receptor (EGFR) family. Here, we addressed the therapeutic potential of the soluble form of Lrig1 (sLrig1) in glioblastoma treatment and the mechanism of sLrig1-induced growth inhibition.
Methods. With use of encapsulated cells, recombinant sLrig1 was locally delivered in orthotopic glioblastoma xenografts generated from freshly isolated patient tumors. Tumor growth and mouse survival were evaluated. The efficacy of sLrig1 and the affected downstream signaling was studied in vitro and in vivo in glioma cells displaying variable expression of wild-type and/or a constitutively active EGFR mutant (EGFRvIII).
Results. Continuous interstitial delivery of sLrig1 in genetically diverse patient-derived glioma xenografts led to strong tumor growth inhibition. Glioma cell proliferation in vitro and tumor growth in vivo were potently inhibited by sLrig1, irrespective of EGFR expression levels. Of importance, tumor growth was also suppressed in EGFRvIII-driven glioma. sLrig1 induced cell cycle arrest without changing total receptor level or phosphorylation. Affected downstream effectors included MAP kinase but not AKT signaling. Of importance, local delivery of sLrig1 into established tumors led to a 32% survival advantage in treated mice.
Conclusions. To our knowledge, this is the first report demonstrating that sLrig1 is a potent inhibitor of glioblastoma growth in clinically relevant experimental glioma models and that this effect is largely independent of EGFR status. The potent anti-tumor effect of sLrig1, in combination with cell encapsulation technology for in situ delivery, holds promise for future treatment of glioblastoma.

Keywords: alginate, cell encapsulation, EGFR, glioblastoma, glioma, Lrig1, tyrosine kinase receptors, xenograft models.

Growth factor signaling through membrane-bound receptor tyrosine kinases (RTKs) regulates major cancer-related processes, including cell proliferation, survival, and invasion. Deregulated growth factor signaling pathways are a hallmark of cancer and an established target for treatment in clinical oncology.[1] In primary glioblastoma (GBM), aberrant RTK signaling is reported in up to 90% of cases, involving aberrations in either the cell surface receptors or their downstream signaling pathways.[2] The receptor genes most commonly mutated or amplified in GBM include epidermal growth factor receptor (*EGFR*; 45%), *ErbB2* (8%), platelet-derived growth factor receptor alpha (*PDGFRA*; 13%), and *MET* (4%).[2] The majority of GBMs with an EGFR gene amplification coexpress a truncated form of the receptor that lacks part of the extracellular domain, the EGFR variant III (EGFRvIII, also known as ΔEGFR).[3] EGFRvIII is unable to bind ligand but signals constitutively and is highly oncogenic.[4]

Received July 26, 2012; accepted March 10, 2013.

†These authors contributed equally to this work.

Corresponding Author: Simone P. Niclou, NorLux Neuro-Oncology Laboratory, CRP-Santé, 84, Val Fleuri, L-1526 Luxembourg, Luxembourg (simone.niclou@crp-sante.lu).

© The Author(s) 2013. Published by Oxford University Press on behalf of the Society for Neuro-Oncology.
This is an Open Access article distributed under the terms of the Creative Commons Attribution License (http://creativecommons.org/licenses/by-nc/3.0/), which permits non-commercial use, distribution, and reproduction in any medium, provided the original work is properly cited. For commercial re-use, please contact journals.permissions@oup.com.

Downloaded from https://academic.oup.com/neuro-oncology/article/15/9/1200/1040732 by Malarsjukhuset user on 23 February 2024

Lrig1 (leucine-rich repeats and immunoglobulin-like domains 1) is a pan-negative regulator of the EGFR receptor family (EGFR and ErbB2-4), inducing downregulation and degradation of the receptors.[5,6] The protein belongs to a family of three structurally similar proteins, including Lrig2 and Lrig3, and is characterized by a large extracellular or luminal domain consisting of leucine-rich repeats (LRR) and three immunoglobulin-like domains, by a transmembrane domain and a cytosolic part.[7–9] Lrig1 was recently identified as a stem cell marker in epidermis, colon, and intestine and regulates stem cell quiescence through tight regulation of ErbB signaling.[10–13] Loss of Lrig1 in mice leads to hyperproliferation in the epidermis and to intestinal neoplasia,[10,11] thus confirming its role as a tumor suppressor gene.[14] The expression of Lrig proteins was previously described in astrocytic and oligodendrocytic brain tumors, where the subcellular localization harbors prognostic information[15,16] (reviewed elsewhere[17]). Lrig1 has also been reported to contain prognostic information in prostate cancer[18] and was recently shown to be an independent positive prognostic factor in estrogen receptor positive breast cancer.[19]

Inhibition of EGFR signaling by Lrig1 results from a physical interaction between the extracellular domain of both proteins, inducing the recruitment of E3 ubiquitin ligases to the cytosolic part of the Lrig1-EGFR complex, followed by internalization and enhanced lysosomal degradation of the protein complex.[5,6] Recently, paracrine regulation of EGFR signaling by shed extracellular Lrig1 was demonstrated to occur naturally; however, the mechanism of action of shed Lrig1 may not involve EGFR protein downregulation.[20] A therapeutic potential for the Lrig1 ectodomain has been proposed.[20,21] In this context, adenoviral delivery of full-length Lrig1 was recently reported to suppress tumor growth in a xenograft model of human bladder cancer.[22] Of interest, Lrig1 also suppresses other RTKs, including MET[23] and RET,[24] and of importance in the glioma context, was shown to negatively regulate EGFRvIII signaling in vitro, although the mechanism of this interaction is currently not entirely clear.[25]

Here, we addressed whether the soluble extracellular part of Lrig1 (sLrig1) is capable of inhibiting glioma growth in vitro and in vivo. In particular, we investigated the effect of sLrig1 in clinically relevant orthotopic GBM xenografts derived from patient tumors with different genetic backgrounds. Using a local delivery system for sLrig1, we demonstrate a potent growth inhibitory effect on patient-derived GBMs resulting in a striking survival benefit in mice with pre-established tumors. Of interest, gliomas with variable expression of EGFR and/or EGFRvIII are strongly inhibited by sLrig1, both in vitro and in vivo, suggesting that the activity of sLrig1 was independent of EGFR status. We further find that sLrig1 regulates cell cycle progression in glioma and inhibits MAP kinase (MAPK) activation. To our knowledge, this is the first report showing the potent inhibitory activity of soluble Lrig1 protein on tumor growth in vivo.

Materials and Methods

Patient Tumor Material

Primary GBM biopsy samples were obtained from the Neurosurgery Department of the Centre Hospitalier in Luxembourg (T16) or the University of Bergen in Norway (P3) after informed consent from the patients.[26] Collection and use of patient tumor tissue samples was approved by the appropriate local ethics committees. GBM spheroids were generated as previously described.[27] In brief, freshly dissected human GBM biopsy samples were minced into 0.3–0.5 mm fragments, which were then cultured in agar-coated tissue culture flasks in serum supplemented DMEM complemented with nonessential amino acids (Cambrex; Lonza, Switzerland). After 8–10 days, spheroids with a diameter of 200–300 μm were selected for intracerebral implantation in mice. Serial transplantation in the brain of enhanced green fluorescent protein (eGFP) expressing NOD/Scid mice was used to expand the tumor material.[28]

Cell Culture

For in vitro and in vivo experiments, the U87 glioblastoma cell line[29] and variants thereof were used: U87 cells overexpressing wild-type EGFR (U87-EGFR) or the truncated and constitutively active EGFR mutant lacking exons 2-7 (U87-EGFRvIII).[30] For cell encapsulation experiments, baby hamster kidney (BHK) cells were used as sLrig1 producer cells. U87 and BHK cells were cultured in Dulbecco's modified Eagle's medium (DMEM) supplemented with 10% fetal calf serum, 100 U/mL penicillin, 100 U/mL streptomycin, and 2 mM glutamine (all from Cambrex; Lonza, Switzerland). Conditioned medium (CM) was collected from confluent BHK control or BHK-sLrig1–producing cells after a 4–7-day incubation period. For EGFR phosphorylation experiments, CM was harvested under serum-free conditions. CM was cleared from cell debris by centrifugation, passed through a 0.2 μm filter, and concentrated by centrifugation through a 100 kDa cutoff filter (Millipore, UFC910024-Amicon).

Lrig1 Constructs, Viral Vector Production, and Cell Transduction

A gene expression construct encoding the extracellular part of human Lrig1 fused to the 3xFLAG epitope (Sigma-Aldrich) was cloned into the pRRL MCS+ lentiviral vector.[31] Lentiviral particles were produced in 293T cells by cotransfection of the pRRL-sLrig1-FLAG vector with the viral core packaging construct pCMVdeltaR8.74 and the VSV-G envelope protein vector pMD.G.2, as previously described.[32] Viral particle-containing cell supernatant was harvested, and titers were determined in 293T cells. The proportion of transduced cells was determined by immunofluorescence labeling of the FLAG epitope (goat anti-FLAG mouse monoclonal antibody; Sigma, F1804) and quantified

Downloaded from https://academic.oup.com/neuro-oncology/article/15/9/1200/1040732 by Malarsjukhuset user on 23 February 2024

using flow cytometry. Lentiviral particles (1×10^6 TU/mL) were used to stably transduce U87 glioma cells and BHK cells with the pRRL-sLrig1-FLAG vector. Transduction efficiency of 90%–98% was obtained as determined by anti-FLAG immunofluorescent staining. Secretion of the sLrig1-FLAG fusion protein into conditioned media of cells and capsules was verified by Western blot analysis.

Generation of Alginate Capsules

Alginate bioreactors were prepared by encapsulating BHK or BHK-sLrig1 cells in alginate polymers as previously described.[33] In brief, subconfluent BHK producer cells were harvested, counted, and mixed with 2% sodium alginate (ultrapure, low viscosity, high guluronic acid content; PRONOVA UP LVG, NovaMatrix - FMC BioPolymer AS, Norway) in a Ca^{2+}-free Krebs-Ringer-Hepes solution (90 mM NaCl, 4.7 mM KCl, 1.2 mM KH_2PO_4, 1.2 mM $MgSO_4$, 25 mM Hepes, pH 7.4) at a concentration of 50×10^6 cells/mL. Beads were generated with an electrostatic bead generator, in which alginate droplets passed a sharpened nozzle of a diameter of 0.17 mm (Nisco Engineering AG, Switzerland). The gelling bath was composed of 100 mM $CaCl_2$, 2 mM KCl, 10 mM Hepes (pH 7.4). A schematic overview of the encapsulation technology and bead production is shown in Supplementary Fig. S1. After encapsulation, the secretion of sLrig1 into the medium was verified by Western blot analysis. Beads with a diameter of 250–300 μm were used for implantation experiments.

In Vivo Tumor Growth and Survival Study

In vivo experiments were performed in female athymic nude (nu/nu) mice (Charles River; Lyon, France). In brief, mice were surgically anesthetized using ketamine 100 mg/kg and xylazin 10 mg/kg. Before skin incision, 100 μL bupivacaine 5 mg/mL was injected into the scalp, and a burr hole was created ~2 mm ventrally of the *sutura coronaria*. The *dura mater* was thereafter carefully punctured, and cells or tumor spheroids suspended in DMEM were stereotactically implanted into the right hemisphere at a depth of 2 mm with use of a 5 μL microsyringe with a 24 gauge needle (Hamilton; Bonaduz, Switzerland) fitted on a stereotactic micromanipulator (Narishige; London, UK). Injection was done slowly, and care was taken not to induce reflux of injected cells when retracting the syringe. The burr hole was closed with bone wax, and the skin incision was closed with sutures. For cell lines, 5×10^4 cells were injected per brain. For alginate bioreactor experiments, 5×10^4 U87, U87-EGFR or U87-EGFRvIII cells were coinjected with 5 alginate beads. For experiments with primary tumors, 5 spheroids were coinjected with 5 alginate beads according to the same protocol. All animals were kept in a controlled environment with a 12-h light/dark cycle and fed *ad libitum*. For each experiment, mice from all groups were sacrificed the same day at the onset of the first neurological symptoms of the control mice (at 3 weeks for U87 tumors, at 4 weeks for T16, and 5 weeks for P3 xenografts). For the survival study, mice were first implanted with GBM spheroids (P3), followed by noninvasive fluorescence imaging to monitor tumor growth (Fig. 5A). After 2 weeks, a clear fluorescent signal was visible and a second surgery was performed to implant 10 sLrig1-producing or control alginate beads ($n = 12$ per group). Mice were monitored daily, and the following criteria were evaluated: (1) loss of more than 10% of body weight, (2) exhibition of strong neurological signs (difficulty ambulating or abnormal movement), (3) increased lordosis, or (4) swollen belly. The above criteria were scored as follows: grade 0 = none, 1 = early, 2 = established, 3 = severe signs. Animals were sacrificed when either 3 criteria with grade 2 or 1 criterion with grade 3 was reached. All animal experiments were approved by the national authorities responsible for animal experimentation.

Tumor Volume Assessment

Final tumor volumes were assessed ex vivo with use of magnetic resonance imaging (MRI). In brief, brains were extracted and fixed in 4% paraformaldehyde. Thereafter, T2-weighted MRI scans (Fast Spin Echo sequences with TE = 11.7 ms, TR = 3600 ms, and 78 μm in plane resolution) were obtained of the entire brain on a 7T micro-MRI for small animals (Bruker PharmaScan) with use of a mouse brain volume coil. The tumors were delineated using the Paravision 5.0 software (Bruker; Ettlingen, Germany), and tumor volumes were calculated using serial coronal sections (U87 tumors) or a combination of axial and coronal sections (primary glioma).

Array CGH Analysis

Genomic DNA was extracted from xenograft tumors with use of the DNeasy Blood and Tissue Kit (Qiagen) according to the manufacturer's instructions. DNA was eluted in water, fragmented to a mean size of 200–500 bp using DNAse I (rDNAse I, Ambion), and labeled using the BioPrime aCGH Genomic Labeling Kit (Invitrogen) and Cy3 and Cy5 dyes, purchased from GE Healthcare, according to standard protocols for Agilent array comparative genomic hybridization (aCGH). Commercially available female DNA pooled from multiple anonymous donors (Promega) was used as a reference for each of the aCGH experiments. Labeled DNA was competitively hybridized to SurePrint G3 Human 2×400k CGH microarrays (Agilent Technologies) according to standard Agilent protocols. The slides were scanned at 3 μm resolution with use of the Agilent High-Resolution Microarray scanner, and the image data were extracted using Feature Extraction (Agilent Technologies). Feature extraction files were imported into Genomic Workbench (Agilent Technologies) for visualization and analysis. Aberrations were called using the ADM2 algorithm with a threshold setting of 25, centralization with threshold of 25, and an aberration filter minProbes = 5 and minAvgAbsLogRatio = 0.45.

Downloaded from https://academic.oup.com/neuro-oncology/article/15/9/1200/1040732 by Malarsjukhuset user on 23 February 2024

Cell Proliferation Assays

Growth curves of U87-EGFRvIII and U87-EGFRvIII-sLrig1 were obtained by plating 1×10^4 cells per well in 6-well plates and harvesting at days 3, 7, 10, and 14. Cells were counted using an automated cell counter (CASY system, Roche Applied Science-Innovatis). All cell proliferation experiments were done in triplicates and repeated at least twice. For co-culture experiments, 5×10^4 sLrig1-producing or nonproducing U87-EGFRvIII cells were plated in the upper compartment of a coculture chamber (Greiner, ThinCert Cell Culture Inserts 6 well, #657610), and 1×10^4 U87, U87-EGFR, or U87-EGFRvIII cells were plated in the lower compartment. Cells were cultivated for 10 days, and the relative cell number in the lower compartment was determined using the Vybrant MTT cell proliferation assay kit (V-13154; Molecular Probes), according to the manufacturer's instructions.

Flow Cytometry

A single-cell suspension of cultured cell lines was obtained by trypsinization (0.25% trypsin, Lonza) at 37°C for 2–3 min. Xenograft brains were minced with scalpels and dissociated with MACS Neural Tissue Dissociation Kit (P) (Miltenyi, 130–092-628) according to the manufacturers' instructions. For cell membrane staining, cells were resuspended in Hank's balanced salt solution w/o Ca^{2+}/Mg^{2+} (HBSS), 2% FBS, and 10 mM HEPES (pH 7.4) buffer (100 μL/test) and incubated using phycoerythrin (PE)–conjugated mouse anti-human EGFR (20 μL/test, clone EGFR.1, BD Biosciences) and LIVE/DEAD Fixable Dead Cell Stains (Invitrogen; 1 μg/mL) for 30 min in the dark. For apoptosis/necrosis test, cells were incubated in binding buffer (2% FBS, 10 mM HEPES [pH 7.4], 140 mM NaCl, and 2.5 mM $CaCl_2$ in HBSS) with the anti-annexin V antibody (10 μL/test, Immunotools) and incubated for 30 min at room temperature in the dark. Propidium iodide (PI; 1 μg/mL; Invitrogen) was added shortly before acquisition. For cell cycle analysis, cells were fixed in 80% cold ethanol and stored at −20°C until analysis. Fixed cells were incubated in PI staining solution (20 μg/mL PI, 0.1% Triton X-100, 200 μg/mL DNAse-free RNAse A in HBSS; 1 mL/test) for 30 min at ambient temperature. Data acquisition was performed with a FACSAria SORP cytometer or a FACSCanto flow cytometer (BD Biosciences) and analyzed with the FlowJo software. T16 and P3 tumor cells in xenografts were recognized as single viable nucleated eGFP-negative cells in contrast to eGFP-positive mouse stromal cells. Gating strategy was as described previously.[34]

Western Blot Analyses

Proteins from cell extracts, conditioned media, or culture supernatants from encapsulated cells were resolved by denaturing gel electrophoresis on 4%–12% NuPAGE Novex 4%–12% Bis-Tris Gel (Invitrogen, Belgium) and transferred to polyvinylidene fluoride membranes (Immobilon-FL, Millipore, France, or Invitrolon, Invitrogen, Belgium). The polyvinylidene fluoride membranes were blocked with 2% ECL Advance blocking agent (GE Healthcare, UK) in Tris-buffered saline containing 0.1% Triton X-100 for at least 1 h. Detection of EGFR and EGFRvIII was obtained with a monoclonal anti-EGFR antibody (Invitrogen, AHR5062) followed by a horseradish peroxidase–conjugated goat anti-mouse antibody (1:150 000; Jackson ImmunoResearch, 115-036-003). For the detection of recombinant FLAG-tagged sLrig1, a goat anti-FLAG mouse monoclonal antibody (Sigma, F1804) was used on the SNAP-i.d. detection system (Millipore, France) according to the manufacturer's instructions. The signal was visualized using the ECL Advance Western blot detection kit (GE Healthcare, UK). ECL image acquisition was performed using an ImageQuant LAS 4010 imaging station, and signals were quantified with ImageQuant TL software (GE Healthcare, Belgium).

For phosphorylation experiments, U87 cells were starved in serum-free DMEM (Lonza) for 72 h before 30 min incubation at 37°C with 20 ng/mL EGF (Provitro) in the presence of serum-free sLrig1 or control-conditioned medium. Cell lysates were analyzed on Western blots with use of the following primary antibodies: pEGFR pY1086 (1:1000, Epitomics: #1139-1), pEGFR pY1068 (1:1000, Cell Signaling: #3777) and pEGFR pT693 (1:1000, Epitomics: #2343-1), MAPK (1:2000, Cell Signaling: #4696), pMAPK p44/p42 (1:1000, Cell Signaling: #9101), AKT1 (1:500, Epitomics: #1081-1), pAKT1 pT308 (1:500, Epitomics: #2214-1), pAKT pS473 (1:2000, Cell Signaling: #4060), actin (1:2000, Chemicon, #MAB1501), and tubulin-ßIII (1:1000, Millipore: #MAB1637). ECL signals were imaged as described above.

Statistics

Data were generally presented as mean ± standard error of the mean (SEM). Comparison of groups in the in vivo experiments was made using one-way analysis of variance in MATLAB 7.12.0 (MathWorks, Inc.). Comparison of groups in the in vitro experiments was made using Student *t* test in Excel. For in vivo studies, a *P* value $<.05$ was considered to be statistically significant, and for in vitro studies, a *P* value $<.01$ was considered to be statistically significant.

Results

Interstitial Delivery of sLrig1 Inhibits Growth of Patient-Derived Glioblastoma Xenografts

It was previously shown that proteolytic cleavage of Lrig1, close to the transmembrane domain, gives rise to a soluble protein fragment (sLrig1) that is capable of inhibiting cell proliferation in a paracrine manner.[20] These results raised the possibility that intracranial delivery of sLrig1 at the tumor site might be used to inhibit glioma growth in vivo. To test this hypothesis, we used

Downloaded from https://academic.oup.com/neuro-oncology/article/15/9/1200/1040732 by Malarsjukhuset user on 23 February 2024

cell encapsulation technology based on alginate polymers to generate bioreactors that stably deliver recombinant proteins in situ over a prolonged period[35,36] (for details on the technology, see also Supplementary Fig. S1). Previously, we have successfully applied this technology to halt cognitive decline in neurodegenerative mice and have shown that encapsulated cells are viable for at least 8 months in vivo.[33] A GFP-expressing BHK producer cell line was stably transduced with the sLrig1 construct and encapsulated in alginate polymers. Secretion of sLrig1 protein was confirmed by Western blot analysis of conditioned media from cells and cell capsules, and cell viability within the capsule was monitored by GFP fluorescence (Fig. 1A and B). To test the effect of sLrig1 in a clinically relevant glioma model, we used orthotopic GBM xenografts generated from patient-derived tumor spheroids. Several such GBM xenograft lines have been established in our laboratory and can be maintained by serial transplantation in rodents, where they have been shown to maintain the phenotypical GBM characteristics and the genetic profile of the original patient tumor.[37–39] Of importance, these xenografts elicit a treatment response to established drugs that is highly similar to those observed in patients.[26] When tumor spheroids from 2 different patients with GBM were coimplanted with alginate bioreactors, we observed a prominent reduction of tumor growth in the presence of sLrig1-producing cells (Fig. 1C). For both xenografts, tumor volume was reduced by about 40% in sLrig1-producing animals, compared with animals carrying control cell capsules (tumor volume: 63% of control for P3 and 59% of control for T16, as assessed by ex vivo MRI). Within 1 to 2 months, control tumors completely filled the implanted hemisphere and invaded the contralateral hemisphere through the *corpus callosum*, while sLrig1-exposed tumors remained considerably smaller (Fig. 1D). Implanted capsules could be visualized in some sections and showed the integration into the brain parenchyma and the retention of the cells in the capsules (Fig. 1D). To determine the genetic profile of the tumors, we performed array CGH, which confirmed that the xenografts carried chromosomal aberrations typical of human GBM (Fig. 1E). Of interest, T16 GBM was characterized by a trisomy of chromosome 7 and EGFR amplification, homozygous deletion of CDKN2A/B on chromosome 9, and hemizygous deletion of chromosome 10, including the PTEN gene. P3 GBM was characterized by a homozygous deletion of the PIK3R1 gene on chromosome 5, trisomy of chromosome 7, homozygous deletion of CDKN2A/B on chromosome 9, and hemizygous deletion of chromosome 10, including the PTEN gene (Fig. 1E). Of note, T16 GBM carried an amplified EGFR gene, leading to receptor levels at the cell surface that were at least 20-fold higher in T16 xenografts than in P3 xenografts (Fig. 1F). Of surprise, as shown in Fig. 1C, the inhibitory effect of sLrig1 was similar in both tumors, despite the pronounced difference in their EGFR expression levels. Taken together, these experiments showed that exogenously delivered sLrig1 inhibited the in vivo growth of genetically divergent primary GBMs, and this effect appeared to be unrelated to EGFR protein level.

Exogenous sLrig1 Affects Glioma Growth in Trans Independent of EGFR Status

To determine to what extent the inhibitory activity of sLrig1 was dependent on EGFR expression and status, we used U87 glioma cells expressing different levels of the wild-type EGFR and/or the mutant variant EGFRvIII (Fig. 2A) in coculture experiments with sLrig1-producing cells. In analogy to the primary GBM xenograft study, sLrig1 suppressed the in vitro growth of U87 cells with or without overexpression of wild-type EGFR (Fig. 2B). Of interest, secreted sLrig1 also led to potent growth inhibition of U87 cells overexpressing EGFRvIII (U87-EGFRvIII) (Fig. 2B). Relative cell numbers of the sLrig1-treated cells were 52% of control for U87 and U87-EGFR cells and 64% of control for U87-EGFRvIII cells (Fig. 2B). Thus, the level and type of EGFR expressed was not crucial for the potent inhibitory effect of sLrig1, suggesting that sLrig1 inhibits glioma cell growth in trans in a manner that is at least partially independent of EGFR type and expression level.

Similarly, coimplantation of sLrig1-producing alginate bioreactors with either of the cell lines U87, U87-EGFR, or U87-EGFRvIII into the mouse brain led to a significant reduction of tumor growth in vivo for all 3 cell types (Fig. 2C). The tumor volume of sLrig1-treated tumors was $46\% \pm 16\%$ for U87, $69\% \pm 11\%$ for U87-EGFR, and $50\% \pm 6\%$ for U87-EGFRvIII of control tumors. Tumor volume was assessed by ex vivo MRI, which also allowed us to visualize the cell capsules in some of the tumors (Fig. 2D). In summary, exogenous delivery of sLrig1 potently inhibited glioma growth in vitro and in vivo, regardless of the level and type of EGFR expression.

sLrig1 Suppresses Glioma Growth by Inhibiting Cell Cycle Progression

To address the mechanism of sLrig1-induced glioma growth inhibition, we overexpressed sLrig1 in the highly proliferative U87-EGFRvIII cell line. Successful gene transduction of U87-EGFRvIII cells by lentiviral sLrig1 expression vectors was verified by immunocytochemistry and Western blotting (Fig. 3A). In this fast-growing cell line, proliferation was dramatically inhibited in the sLrig1-overexpressing cells, compared with mock transduced cells (Fig. 3B). The cell doubling time was 1.7 days for control cells and 2.8 days for sLrig1-expressing cells. The growth inhibitory effect of sLrig1 was more pronounced in the transduced cells (Fig. 3B) than in the cells that were exposed to exogenously added sLrig1 (Fig. 2B), a difference that might be explained by different levels of sLrig1 exposure in the 2 systems. Of importance, sLrig1 overexpression led to almost complete growth inhibition in vivo after intracerebral implantation of U87-EGFRvIII cells in nude mice (Figs. 3C–F). After 3 weeks, control animals implanted with U87-EGFRvIII cells displayed large tumors extending throughout the whole right hemisphere, and animals implanted with U87-EGFRvIII-sLrig1 cells displayed barely visible tumors (Figs. 3D–F). Mean tumor volume of control

Downloaded from https://academic.oup.com/neuro-oncology/article/15/9/1200/1040732 by Malarsjukhuset user on 23 February 2024

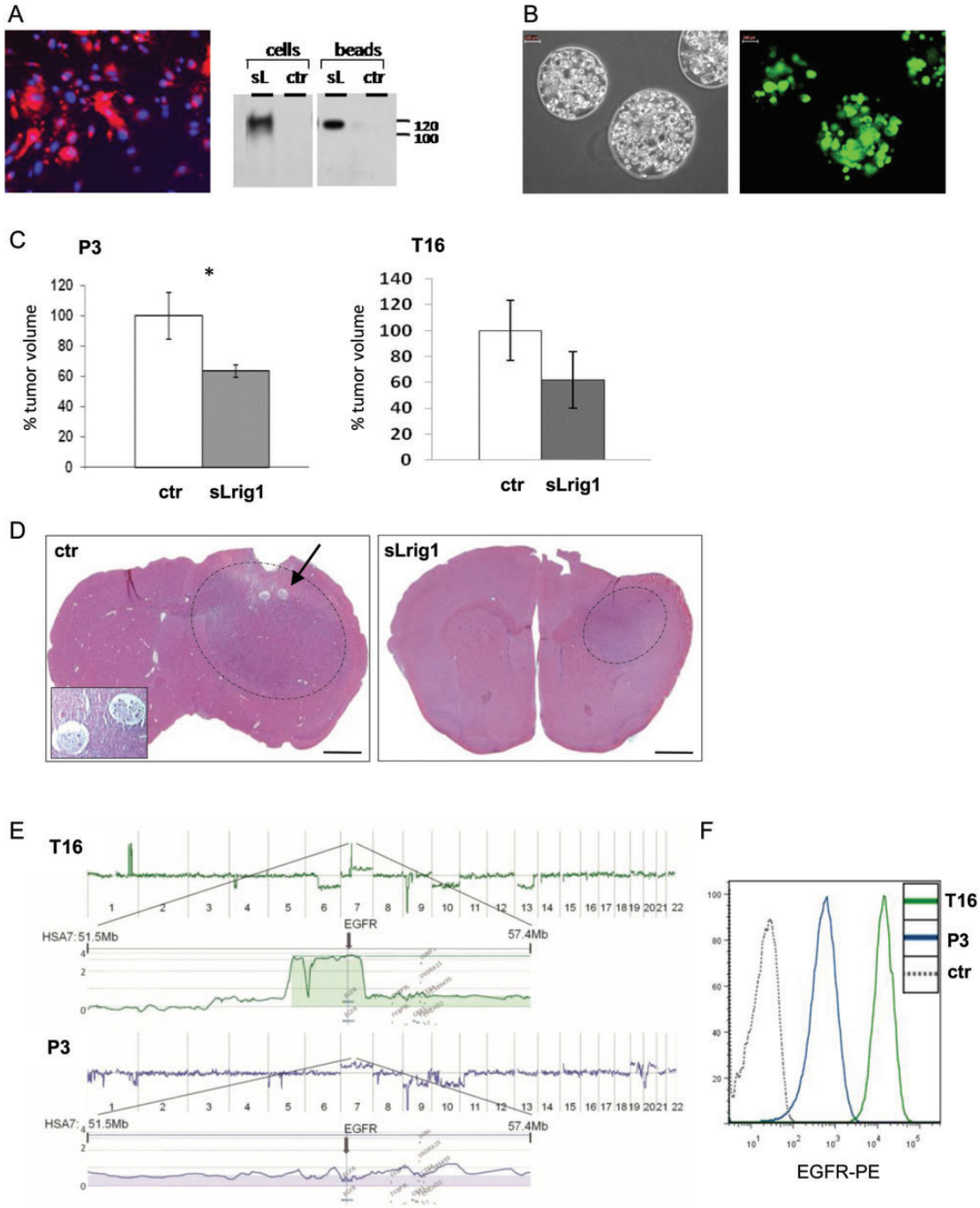

Fig. 1. sLrig1 inhibits in vivo growth of patient-derived GBM xenografts with different genetic profiles. (A) Left panel: Immunofluorescence staining with anti-FLAG antibody (red) of BHK cells stably transduced with the sLrig1 construct. Cell nuclei were counterstained with DAPI (blue). Right panel: Western blot with anti-FLAG antibody detecting sLrig1 at 110 kD in conditioned medium of BHK cells and of corresponding alginate beads (sL: BHK-sLrig1 cells and ctr: BHK control cells). (B) Photomicrograph of BHK cells encapsulated in alginate bioreactors with a diameter of 250–300 μm. Left: phase contrast image, right: GFP fluorescence of encapsulated cells. Scale bar, 100 μm. (C) Coimplantation experiment in the brain of nude mice using 5 organotypic tumor spheroids from either P3 (left) or T16 GBM (right) together with 5 alginate beads containing either sLrig1-producing cells (sLrig1) or control cells (ctr). Tumor volumes were determined by MRI. About 40% growth inhibition was observed in the presence of sLrig1 in both of the patient-derived GBM xenografts. Results are given as percentage of control. Error bars indicate SEM ($n = 6$; $^*P < .05$). (D) Histological sections of P3 xenografts stained with hematoxylin and eosin. In the control tumor section (ctr), the implanted beads are clearly visible (arrow and blow-up). Scale bar, 1 mm. (E) Array CGH profile of T16 and P3 GBM xenografts. Chromosome number is indicated (1–22). Although both tumors carry a trisomy of chromosome 7, only T16 has an amplification of the EGFR gene (blow-up of chromosome 7). (F) Flow cytometric analysis of EGFR on T16 and P3 tumor cells demonstrating high EGFR levels in T16 tumor (x axis: PE fluorescence intensity, y axis: number of cells, ctr: negative control, without antibody).

Downloaded from https://academic.oup.com/neuro-oncology/article/15/9/1200/1040732 by Malarsjukhuset user on 23 February 2024

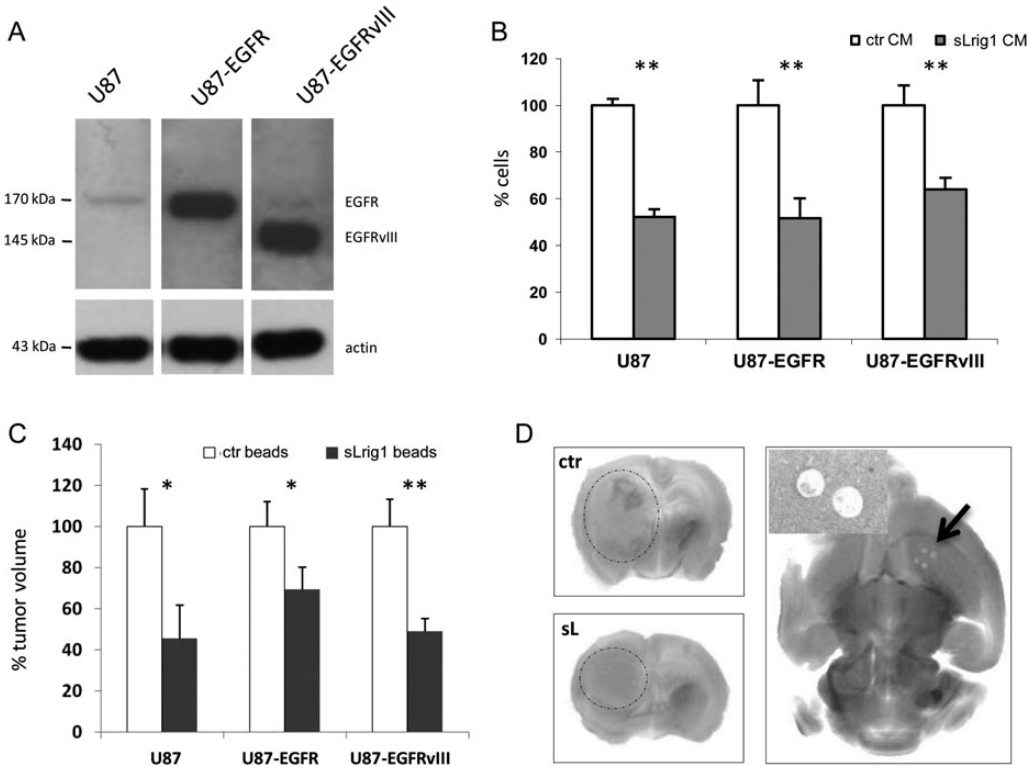

Fig. 2. Exposure to sLrig1 inhibits U87 cell growth in vitro and in vivo, irrespective of EGFR status. (A) Western blot showing the levels of EGFR (at 170 kD) or EGFRvIII (at 145 kD) protein in the 3 U87-derived cell lines under study. Actin (at 43 kD) is shown as a loading control. (B) Coculture experiment showing decreased proliferation of U87, U87-EGFR, and U87-EGFRvIII cells in the presence of sLrig1-producing cells, plated in a cell culture chamber insert. MTT assay was performed at day 10 of culture; cell number is expressed as the percentage of control (x axis). Error bars indicate SEM. $^{**}P < .01$ (*t* test). (C) In vivo growth of U87 cell lines coimplanted with alginate beads in the mouse brain (50 000 tumor cells and 5 beads). Beads contained either control BHK cells (ctr beads) or sLrig1-producing BHK cells (sLrig1 beads). Six mice were used per condition. Tumor volume was defined on consecutive MR images taken 21 days after implantation and expressed as percentage of control. Error bars indicate SEM. $^{*}P < .05$ and $^{**}P < .01$. (D) Representative MR images of control (ctr) and sLrig1 (sL) bead containing brains with U87-EGFRvIII tumors at day 21. The tumor area is demarcated by a dotted line. Right panel shows a horizontal MR image, where alginate beads are clearly visible (arrow). The beads can also be seen on a histological section (inset).

tumors was 89 ± 9.7 mm^3 ($n = 5$), compared with 1.7 ± 0.4 mm^3 for U87-EGFRvIII-sLrig1 tumors ($n = 5$, $P < .01$), as assessed by ex vivo MRI (Fig. 3C). Histological sections indicated that sLrig1 did not affect tumor take (all animals displayed small tumors) and did not appear to induce massive tumor necrosis (Figs. 3E and F). sLrig1-containing tumors displayed a limited number of blood vessels, compared with control tumors (Fig. 3E and F), which is likely to be related to the reduced tumor size. To further address the mechanism of sLrig1-induced growth inhibition, we analyzed the effect of sLrig1 on cell death and cell cycle regulation in vitro. No increase in either apoptotic (annexin V staining) or necrotic (PI staining) cell death was observed in sLrig1-expressing cells (Fig. 3G). However, a significant reduction in the number of cells in the S and G2/M phase of the cell cycle and an accumulation of cells in the G1/G0 phase was observed (Fig. 3H). These data indicate that sLrig1-induced growth inhibition of U87-EGFRvIII cells was mediated by suppression of cell cycle progression.

sLrig1 Exposure Does Not Affect EGFR Protein Level or Receptor Activation Status, but Engages MAPK Signaling

Because our data suggested that the activity of sLrig1 did not correlate to EGFR status of the cells and earlier work had indicated that short-term exposure to sLrig1 was not accompanied by EGFR degradation,[20] we addressed whether sLrig1 affected EGFR protein levels in glioma cells. The different U87 cell lines were exposed to sLrig1 for up to 8 days, corresponding to a time point at which the inhibitory effect of sLrig1 was clearly measurable in the proliferation assay (Fig. 3B). As shown in Fig. 4A, no significant change in total EGFR or EGFRvIII protein level could be detected either at day 1 or at day 8 of sLrig1 exposure in any of the 3 cell lines. We then asked whether the cell surface expression of EGFR might be affected through sLrig1-induced receptor internalization, in a manner that might not be reflected by total protein analysis. Using flow cytometry for cell surface staining of EGFR on living cells, however, we did not detect any change in the number of extracellular EGFR epitopes after sLrig1 exposure (Fig. 4B). We further analyzed the

Downloaded from https://academic.oup.com/neuro-oncology/article/15/9/1200/1040732 by Malarsjukhuset user on 23 February 2024

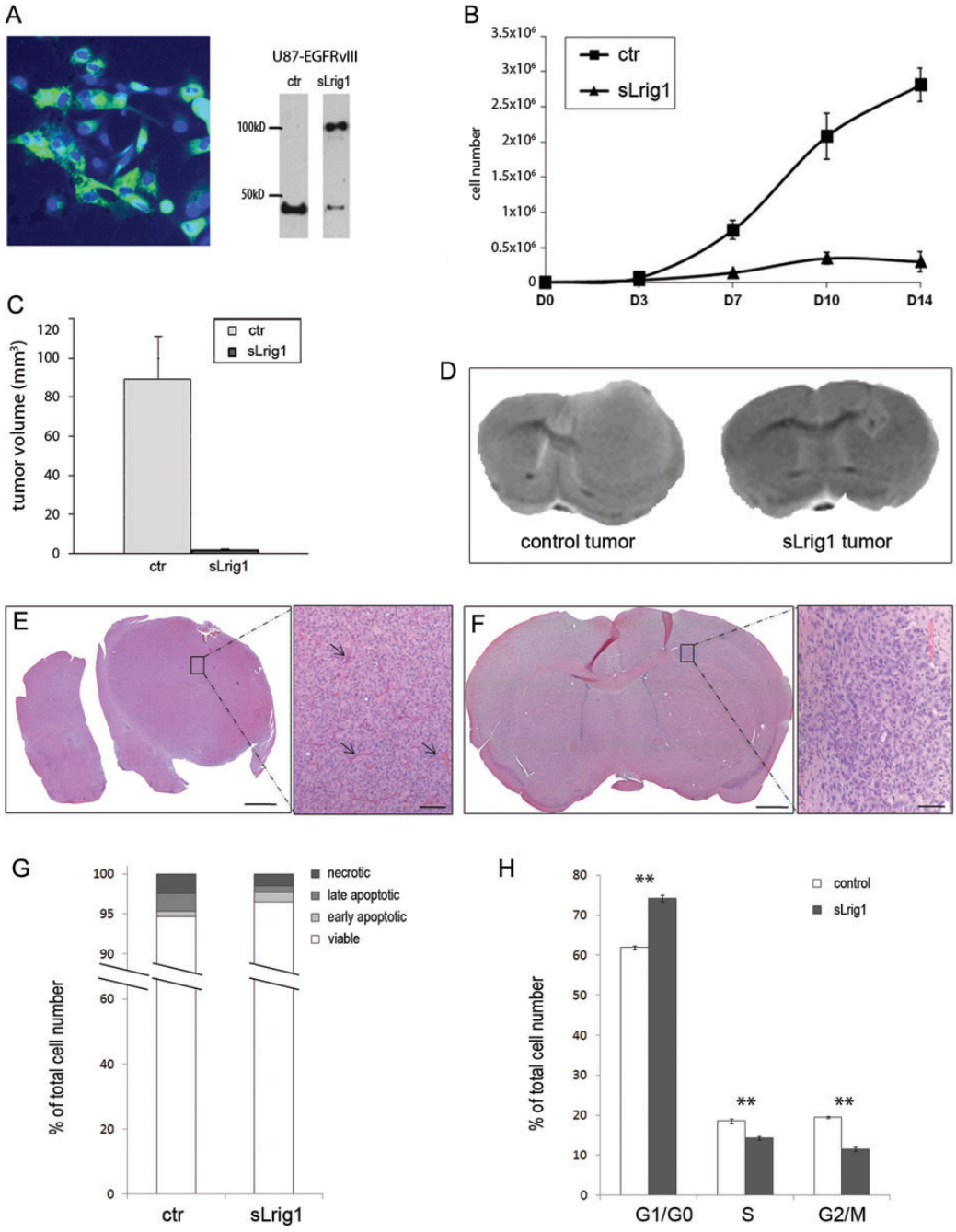

Fig. 3. Overexpression of sLrig1 in U87-EGFRvIII cells potently inhibits growth in vitro and in vivo by induction of cell cycle arrest. (A) Left sLrig1 immunofluorescence staining (green) of U87-EGFRvIII cells overexpressing sLrig1. Cell nuclei were counterstained with DAPI (blue). Right: Western blot with anti-FLAG antibody on lysates of U87-EGFRvIII control cells (ctr) or sLrig1-overexpressing cells (sLrig1), detecting the sLrig1-FLAG fusion protein at 110 kD. Actin is shown for comparison (43 kD). (B) Cell proliferation assay with U87-EGFRvIII (ctr) and U87-EGFRvIII-sLrig1 cells (sLrig1), showing a dramatic growth inhibition of sLrig1 expressing cells. Cell number was counted at indicated time points. Error bars indicate SEM. (C) Quantification of tumor volume after implantation of U87-EGFRvIII (ctr) and U87-EGFRvIII-sLrig1 (sLrig1) in the mouse brain. Tumor volume was defined on consecutive MR images at 21 days after implantation ($n = 5$ per group). Error bars indicate SEM ($P < .01$, t test). (D) Representative MR images showing an extensive tumor in the brain of a U87-EGFRvIII–transplanted mouse (ctr) and a tiny tumor in the brain of a U87-EGFRvIII-sLrig1– transplanted mouse (sLrig1). (E and F) Hematoxylin and eosin–stained histological sections of U87-EGFRvIII (E) and U87-EGFRvIII-sLrig1 (F) tumors (scale bar = 1 mm), with a high magnification view of the highlighted quadrant on the right (scale bar = 100 μm). Arrows in the inset point to blood vessels. (G) Determination of cell death by flow cytometry using annexin V staining for apoptotic cells and PI staining for necrotic cells. Total cell number was set to 100%. (H) Effect of sLrig1 on cell cycle progression was determined by PI staining of fixed U87-EGFRvIII (control) and U87-EGFRvIII-sLrig1 (sLrig1) cells. G1/G0, S, and G2/M indicate phases of the cell cycle (**$P < .001$).

Downloaded from https://academic.oup.com/neuro-oncology/article/15/9/1200/1040732 by Malarsjukhuset user on 23 February 2024

phosphorylation status of EGFR and EGFRvIII in the presence of sLrig1 with use of antibodies against major EGFR phosphorylation sites (pY1068, pY1086, and pT693). As shown on Fig. 4C, stimulation with EGF of serum-starved cells enhanced the phosphorylation of the 3 phospho-sites in U87, U87-EGFR, and U87-EGFRvIII cells, but the phosphorylation levels were not affected by the presence of sLrig1. Of interest, EGF-induced phosphorylation of the downstream effector MAPK was inhibited in the presence of sLrig1, whereas AKT1 phosphorylation was unaffected (Fig. 4D). Taken together, these data showed that inhibition of cell proliferation by sLrig1 in U87 cell lines displaying variable levels of EGFR and/or EGFRvIII was not accompanied by a reduction of EGFR expression level and/or phosphorylation. However, sLrig1 reduced the phosphorylation of the intracellular signal transducer MAPK.

In Situ Delivery of sLrig1 Increases Survival of Mice With Established Orthotopic Patient-Derived Glioblastoma

Finally, we aimed to address whether sLrig1 was capable of improving survival among mice carrying already established GBM xenografts. To this aim, mice were implanted with DsRed-labeled organotypic GBM spheroids (P3), and tumors were allowed to establish themselves. Mice were followed by in vivo fluorescence imaging during the first 2 weeks, until a clear fluorescent signal was obtained indicating successful tumor take (Fig. 5A). A second operation was then performed to implant the alginate capsules containing control or sLrig1-producing cells. This closely mimics the clinical situation in which bioreactors could be implanted during the surgical removal of the tumor, although in this case, we did not

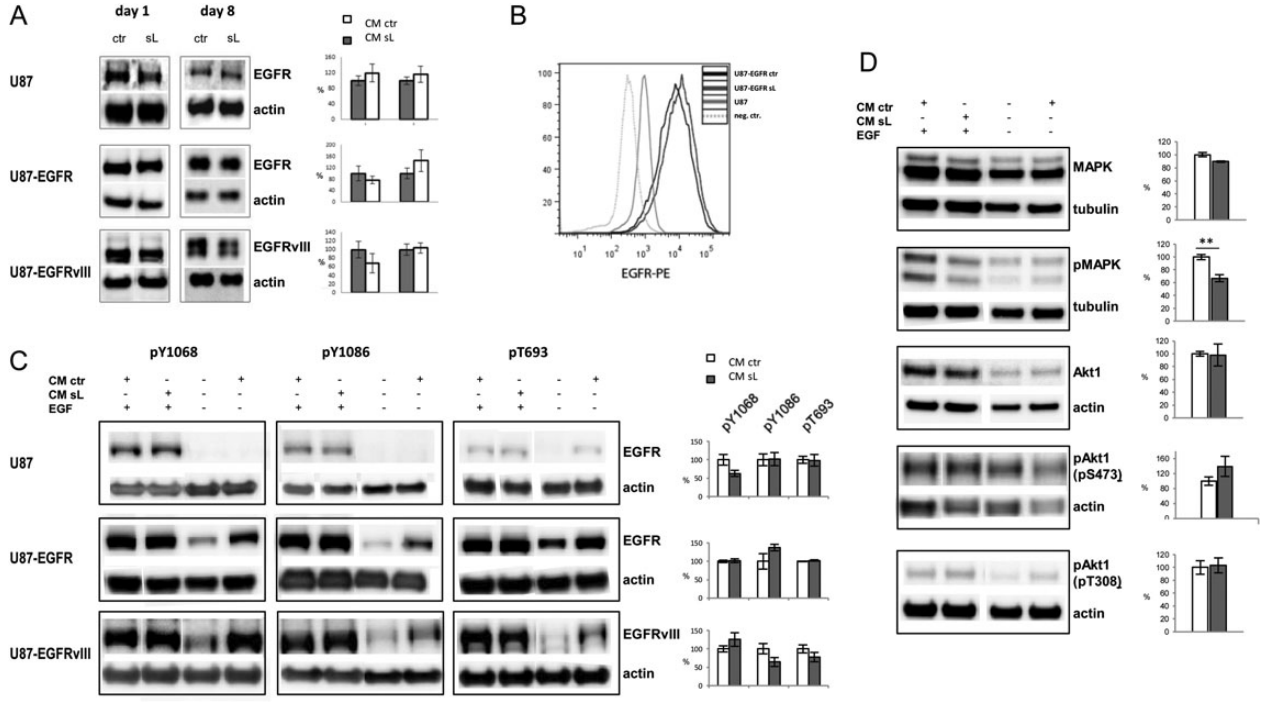

Fig. 4. sLrig1 reduces MAP kinase phosphorylation, but not EGFR or AKT phosphorylation. (A) U87, U87-EGFR, and U87-EGFRvIII cells were incubated for 1 or 8 days with conditioned medium of control cells (CM ctr) or sLrig1-producing cells (CM sL). Western blot analysis with anti-pan EGFR and anti-actin antibodies, indicating that the total receptor level was unchanged after sLRIG1 treatment, at both time points and in all 3 cell lines. Graphs on the right show the relative quantification of receptor levels from 3 independent experiments performed in triplicates. After normalization against actin level, values were expressed as percentage of control (set to 100%, grey bar) to allow compilation of different experiments in one graph. No statistically significant difference was observed. (B) Flow cytometric analysis with PE-labeled anti-EGFR antibody of U87-EGFR cells treated with control (ctr) or sLrig1 (sL)–containing medium. No difference in cell surface expression of EGFR was detected. U87 cells without EGFR overexpression are shown for comparison. Negative control (neg ctr) represents signal in the absence of antibody. (C) After serum starvation, cells were coincubated with 20 ng/mL EGF and sLrig1 for 30 min, followed by Western blot analysis with antibodies specific for major phospho-tyrosine (pY1086, pY1068) and phospho-threonine (pT693) residues on EGFR. Control lanes are shown without EGF stimulation. No significant changes in the phosphorylation level of any of the phosphorylation sites of EGFR or EGFRvIII were detected after sLRIG1 exposure in any of the cell lines. Quantification of signal intensities (right panels) show control (ctr) and sLrig1 (sL)–exposed samples after stimulation with EGF. Values were obtained from at least 2 independent experiments performed in triplicates. (D) Analysis of total protein level and phosphorylation status of MAP kinase (MAPK) and AKT1 after sLrig1 exposure in U87-EGFR cells. Although total protein levels were unchanged for both MAPK and AKT1, only the phosphorylation of MAPK was significantly decreased after sLRIG1 treatment (P value $< .05$). Right panels show the quantification of corresponding blots (as under C), where either tubulin or actin was used as a loading control.

Downloaded from https://academic.oup.com/neuro-oncology/article/15/9/1200/1040732 by Malarsjukhuset user on 23 February 2024

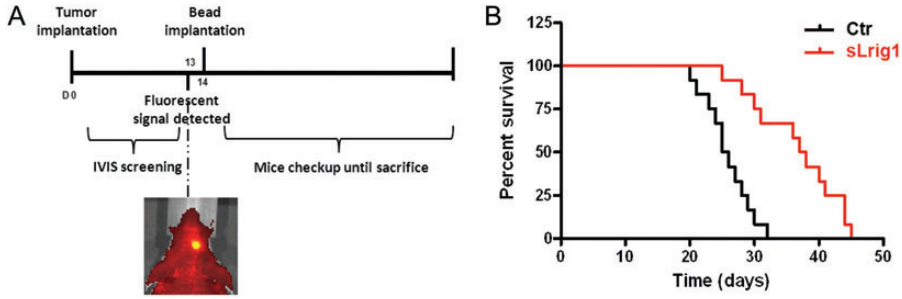

Fig. 5. sLrig1 increases survival of glioma-bearing mice. (A) Experimental setup of survival study. Patient-derived organotypic GBM spheroids (P3) expressing DsRed were implanted into the brain of mice at day 0 (D0) and followed by fluorescence monitoring (IVIS screening) 3 times a week. At day 13, a clear tumor signal was detected, and at day 14, the animals underwent a second surgery for alginate bioreactor implantation. Mice were checked for neurological symptoms until sacrifice. (B) Kaplan-Meier survival plot of mice treated with control (Ctr) or sLrig1-secreting alginate beads. A median survival benefit of 12 days was observed in the experimental group (25.5 vs 37.5 days; $n = 12$ mice per group; $P < .001$). Days are indicated from the time of treatment.

remove the already established tumor. Mice were followed by careful monitoring over the next weeks and sacrificed on the basis of a predefined scoring system (see Materials and Methods). Median survival among control mice was 25.5 days, and that among sLrig1-producing mice was 37.5 days from start of treatment, indicating an increase in survival of 12 days for the treated mice (32%) (Fig. 5B). These data demonstrate that sLrig1 is not only active on tumor establishment, but strongly affects tumor progression of already established tumors, suggesting that the approach presented here holds promise for postoperative in situ adjuvant therapy of patients with GBM.3

Discussion

In the present study, we showed that interstitial delivery of the soluble extracellular part of Lrig1, sLrig1, potently inhibits glioma growth in vivo. Of importance, this inhibitory effect was equally observed in several glioma models, including clinically relevant patient-derived GBM xenografts, irrespective of the EGFR gene amplification status of the tumor. Growth was inhibited in tumors expressing barely detectable levels of EGFR and in tumors overexpressing wild-type EGFR or the constitutively active EGFRvIII mutant, suggesting that the effect is at least partially independent of ligand activation or the type and level of EGFR expression. The inhibitory effect of sLrig1 not only was limited to tumor establishment but also potently reduced tumor progression of established GBM xenografts, leading to a 32% survival benefit among treated mice. To our knowledge, this is the first time that a potent in vivo anti-tumor effect of sLrig1 and a positive effect on survival has been demonstrated.

What Is the Mechanism of Action of sLrig1?

The recombinant leucine-rich repeat (LRR) domain of Lrig1 has previously been shown to attenuate EGFR signaling by acting as a competitive inhibitor for EGF binding.[21] In that study, Lrig-LRR inhibited growth of EGFR-expressing carcinoma cells but failed to inhibit growth of cells not expressing EGFR. This is in contrast to our findings in which sLrig1, containing the LRR and immunoglobulin-like domains, was equally effective in inhibiting cell proliferation irrespective of EGFR expression level and ligand activation. Indeed, in agreement with a previous report on transmembrane Lrig1,[25] we showed that sLrig1 suppressed cell proliferation and tumor growth also in cells expressing the constitutively active EGFRvIII mutant, which is unable to bind any known ligand. Furthermore, we did not see an effect of sLrig1 on ligand-induced phosphorylation of EGFR. Taken together, our results suggest that the inhibitory activity of sLrig1 cannot be simply explained by its potential to interfere with EGF binding.

The originally described mechanism of action of full-length transmembrane Lrig1 is downregulation of the steady state level of the EGFR family members by inducing ubiquitinylation and subsequent lysosomal degradation of the protein complex.[5,6] sLrig1 on the other hand has been reported in short-term experiments to inhibit c-fos induction without affecting EGFR levels.[20] These data are extended in the present study, in which we did not detect a reduction in EGFR protein levels or internalization even after long-term treatment with sLrig1 (up to 8 days), neither did we observe any effect on the activation status of the receptor. Of interest, we observed that sLrig1 induced cell cycle arrest and led to a reduction of MAPK but not AKT phosphorylation, suggesting an involvement of the MAPK pathway in sLrig1-induced cell cycle arrest. This is in line with the previously reported suppression of c-fos induction, a downstream target of MAPK.[20] However, it is currently not clear by which mechanism MAPK activation was inhibited in our experiments.

Because sLrig1 was equally potent on glioma cells independent of their EGFR status and EGFR levels, we cannot rule out that sLrig1-mediated inhibition of cell proliferation and tumor growth does not exclusively rely on EGFR signaling. sLrig1 might interact with other RTKs on glioma cells or act through an RTK-independent mechanism. It was recently reported that

Downloaded from https://academic.oup.com/neuro-oncology/article/15/9/1200/1040732 by Malarsjukhuset user on 23 February 2024

transmembrane Lrig1 can suppress estrogen-driven breast cancer cell proliferation in vitro,[19] a process that is not believed to be dependent on RTKs. It remains to be seen whether sLrig1 directly interacts with an as yet unidentified receptor on the cell surface to induce intracellular signaling. In this respect, it is important to note that Lrig1 can be proteolytically cleaved by endogenous proteases and released into the extracellular space,[20] raising the possibility that endogenous sLrig fragments may function as important paracrine and physiological regulators in vivo.

sLrig1: A Novel Glioma Treatment?

In malignant glioma, the clinical outcome after treatment with RTK inhibitors has been largely disappointing thus far.[40] One of the explanations for the failure of these drugs in neuro-oncology may be linked to the redundancy of RTK signaling in glioma.[2] The fact that Lrig1 regulates multiple RTK pathways and our data showing that sLrig1 induces cell cycle arrest in cells with variable EGFR status raises the possibility that sLrig1 could serve as an efficient global inhibitor of RTK signaling and glioma growth. We observed a sLrig1-mediated growth inhibition of about 40% in patient-derived GBMs, independent of their genetic background, strongly suggesting that sLrig1 has the potential to function as a novel and highly potent therapeutic agent against malignant glioma, particularly against the aggressive EGFRvIII-expressing tumors. Of note, in this context, sLrig1-induced growth arrest was observed despite the loss of the PTEN tumor suppressor gene in the tumors. In this respect, it will be important to further elucidate the mechanism of action of sLrig1 and determine the minimal protein domain required for its inhibitory activity.

Another major challenge in neuro-oncology is the poor penetration of drugs into the tumor site because of the blood-brain barrier and a high intra-tumoral pressure gradient. Alginate polymer-based cell capsules provide local and long-term secretion of the therapeutic protein directly to the tumor core and represent a valid therapeutic strategy for the treatment of primary brain tumors, especially in the adjuvant setting, where alginate beads could be injected into the walls of the resection cavity.[35,41] The growth inhibition obtained here was based on only 5 capsules implanted per brain, corresponding to about 2–3000 producer cells. Increasing the number of implanted capsules harbors the potential to increase the therapeutic effect.

To conclude, we report for the first time that interstitial delivery of the extracellular part of Lrig1 potently increases survival of glioma-bearing mice and inhibits glioma growth in vitro and in vivo by regulating cell cycle progression. We believe that cell-based delivery of macromolecules inhibiting growth factor signaling is a promising strategy for loco-regional postoperative adjuvant treatment in GBM and sLrig1 is a promising therapeutic candidate to further evaluate.

Supplementary Material

Supplementary material is available online at *Neuro-Oncology* (http://neuro-oncology.oxfordjournals.org/).

Acknowledgments

We thank Vanessa Barthelemy and Virginie Baus for invaluable technical support. U87-EGFR and U87-EGFRvIII cells were kindly provided by Dr. F. Furnari and Prof. W. Cavenee from the Ludwig Institute in La Jolla, CA.

Funding

This work was supported by the Fonds National de la Recherche of Luxembourg through the CORE program (ENCAPS project C08/BM/11 to S.P.N.). M.J. was cofunded by the Cancer Research Foundation in Northern Sweden and the Department of Oncology, Umeå University Hospital, Sweden.

Conflict of interest statement. None declared.

References

1. Palazzo A, Iacovelli R, Cortesi E. Past, present and future of targeted therapy in solid tumors. *Current Cancer Drug Targets*. 2010;10:433–461.
2. Network CGAR. Comprehensive genomic characterization defines human glioblastoma genes and core pathways. *Nature*. 2008;455:1061–1068.
3. Ekstrand AJ, Sugawa N, James CD, et al. Amplified and rearranged epidermal growth factor receptor genes in human glioblastomas reveal deletions of sequences encoding portions of the N- and/or C-terminal tails. *Proc Natl Acad Sci USA*. 1992;89:4309–4313.
4. Hatanpaa KJ, Burma S, Zhao D, et al. Epidermal growth factor receptor in glioma: signal transduction, neuropathology, imaging, and radioresistance. *Neoplasia*. 2010;12:675–684.
5. Gur G, Rubin C, Katz M, et al. LRIG1 restricts growth factor signaling by enhancing receptor ubiquitylation and degradation. *EMBO J*. 2004;23:3270–3281.
6. Laederich MB, Funes-Duran M, Yen L, et al. The leucine-rich repeat protein LRIG1 is a negative regulator of ErbB family receptor tyrosine kinases. *J Biol Chem*. 2004;279:47050–47056.
7. Guo D, Holmlund C, Henriksson R, et al. The LRIG gene family has three vertebrate paralogs widely expressed in human and mouse tissues and a homolog in Ascidiacea. *Genomics*. 2004;84:157–165.
8. Holmlund C, Nilsson J, Guo D, et al. Characterization and tissue-specific expression of human LRIG2. *Gene*. 2004;332:35–43.

Downloaded from https://academic.oup.com/neuro-oncology/article/15/9/1200/1040732 by Malarsjukhuset user on 23 February 2024

9. Nilsson J, Vallbo C, Guo D, et al. Cloning, characterization, and expression of human LIG1. *Biochemical and Biophysical Research Communications*. 2001;284:1155–1161.
10. Jensen KB, Collins CA, Nascimento E, et al. Lrig1 expression defines a distinct multipotent stem cell population in mammalian epidermis. *Cell Stem Cell*. 2009;4:427–439.
11. Powell AE, Wang Y, Li Y, et al. The pan-ErbB negative regulator Lrig1 is an intestinal stem cell marker that functions as a tumor suppressor. *Cell*. 2012;149:146–158.
12. Wong VW, Stange DE, Page ME, et al. Lrig1 controls intestinal stem-cell homeostasis by negative regulation of ErbB signalling. *Nat Cell Biol*. 2012;14:401–408.
13. Suzuki Y, Miura H, Tanemura A, et al. Targeted disruption of LIG-1 gene results in psoriasiform epidermal hyperplasia. *FEBS Lett*. 2002;521:67–71.
14. Hedman H, Nilsson J, Guo D, et al. Is LRIG1 a tumour suppressor gene at chromosome 3p14.3?. *Acta Oncol*. 2002;41:352–354.
15. Guo D, Nilsson J, Haapasalo H, et al. Perinuclear leucine-rich repeats and immunoglobulin-like domain proteins (LRIG1–3) as prognostic indicators in astrocytic tumors. *Acta Neuropathol*. 2006;111:238–246.
16. Holmlund C, Haapasalo H, Yi W, et al. Cytoplasmic LRIG2 expression is associated with poor oligodendroglioma patient survival. *Neuropathology*. 2009;29:242–247.
17. Hedman H, Henriksson R. LRIG inhibitors of growth factor signalling - double-edged swords in human cancer?. *Eur J Cancer*. 2007;43:676–682.
18. Thomasson M, Wang B, Hammarsten P, et al. LRIG1 and the liar paradox in prostate cancer: a study of the expression and clinical significance of LRIG1 in prostate cancer. *Int J Cancer*. 2011;128:2843–2852.
19. Krig SR, Frietze S, Simion C, et al. Lrig1 is an estrogen-regulated growth suppressor and correlates with longer relapse-free survival in ERalpha-positive breast cancer. *Mol Cancer Res*. 2011;9:1406–1417.
20. Yi W, Holmlund C, Nilsson J, et al. Paracrine regulation of growth factor signaling by shed leucine-rich repeats and immunoglobulin-like domains 1. *Exp Cell Res*. 2011;317:504–512.
21. Goldoni S, Iozzo RA, Kay P, et al. A soluble ectodomain of LRIG1 inhibits cancer cell growth by attenuating basal and ligand-dependent EGFR activity. *Oncogene*. 2007;26:368–381.
22. Li F, Ye ZQ, Guo DS, et al. Suppression of bladder cancer cell tumorigenicity in an athymic mouse model by adenoviral vector-mediated transfer of LRIG1. *Oncol Rep*. 2011;26:439–446.
23. Shattuck DL, Miller JK, Laederich M, et al. LRIG1 is a novel negative regulator of the Met receptor and opposes Met and Her2 synergy. *Mol Cell Biol*. 2007;27:1934–1946.
24. Ledda F, Bieraugel O, Fard SS, et al. Lrig1 is an endogenous inhibitor of Ret receptor tyrosine kinase activation, downstream signaling, and biological responses to GDNF. *J Neurosci*. 2008;28:39–49.
25. Stutz MA, Shattuck DL, Laederich MB, et al. LRIG1 negatively regulates the oncogenic EGF receptor mutant EGFRvIII. *Oncogene*. 2008;27:5741–5752.
26. Keunen O, Johansson M, Oudin A, et al. Anti-VEGF treatment reduces blood supply and increases tumor cell invasion in glioblastoma. *Proc Natl Acad Sci U S A*. 2011;108:3749–3754.
27. Bjerkvig R, Tonnesen A, Laerum OD, et al. Multicellular tumor spheroids from human gliomas maintained in organ culture. *J Neurosurg*. 1990;72:463–475.
28. Niclou SP, Danzeisen C, Eikesdal HP, et al. A novel eGFP-expressing immunodeficient mouse model to study tumor-host interactions. *Faseb J*. 2008;22(9):3120–3128.
29. Ponten J, Macintyre EH. Long term culture of normal and neoplastic human glia. *Acta Pathol Microbiol Scand*. 1968;74:465–486.
30. Nishikawa R, Ji XD, Harmon RC, et al. A mutant epidermal growth factor receptor common in human glioma confers enhanced tumorigenicity. *Proc Natl Acad Sci USA*. 1994;91:7727–7731.
31. Naldini L, Blomer U, Gallay P, et al. In vivo gene delivery and stable transduction of nondividing cells by a lentiviral vector. *Science*. 1996;272:263–267.
32. Ahmed BY, Chakravarthy S, Eggers R, et al. Efficient delivery of Cre-recombinase to neurons in vivo and stable transduction of neurons using adeno-associated and lentiviral vectors. *BMC Neurosci*. 2004;5:4.
33. Garcia P, Youssef I, Utvik JK, et al. Ciliary neurotrophic factor cell-based delivery prevents synaptic impairment and improves memory in mouse models of Alzheimer's disease. *J Neurosci*. 2010;30:7516–7527.
34. Golebiewska A, Brons NH, Bjerkvig R, et al. Critical appraisal of the side population assay in stem cell and cancer stem cell research. *Cell Stem Cell*. 2011;8:136–147.
35. Niclou SP, Bjerkvig R. Treatment of brain tumors with micro-encapsulated cell therapy, In: Hallé, J.P. dVP, Rosenberg, L. ed. *The Bioartificial Pancreas and other Biohybrid Therapies*. Canada: Research Signpost, 2009.
36. Visted T, Bjerkvig R, Enger PO. Cell encapsulation technology as a therapeutic strategy for CNS malignancies. *Neuro Oncol*. 2001;3:201–210.
37. Rajcevic U, Petersen K, Knol JC, et al. iTRAQ-based proteomics profiling reveals increased metabolic activity and cellular cross-talk in angiogenic compared with invasive glioblastoma phenotype. *Mol Cell Proteomics*. 2009;8:2595–2612.
38. Sakariassen PO, Prestegarden L, Wang J, et al. Angiogenesis-independent tumor growth mediated by stem-like cancer cells. *Proc Natl Acad Sci USA*. 2006;103:16466–16471.
39. Wang J, Miletic H, Sakariassen PO, et al. A reproducible brain tumour model established from human glioblastoma biopsies. *BMC Cancer*. 2009;9:465.
40. De Witt Hamer PC. Small molecule kinase inhibitors in glioblastoma: a systematic review of clinical studies. *Neuro-Oncology*. 2010;12:304–316.
41. Read TA, Sorensen DR, Mahesparan R, et al. Local endostatin treatment of gliomas administered by microencapsulated producer cells. *Nat Biotechnol*. 2001;19:29–34.

Downloaded from https://academic.oup.com/neuro-oncology/article/15/9/1200/1040732 by Malarsjukhuset user on 23 February 2024